Chapter published in *Macromolecular Engineering: From Precise Synthesis to Macroscopic Materials and Applications*, 2nd edition, edited by Krzysztof Matyjaszewski, Yves Gnanou, Nikos Hadjichristidis, Murugappan Muthukumar (Wiley-VCH GmbH, 2022)

This article may be found at https://doi.org/10.1002/9783527815562.mme0064

Chapter
Polymer Glasses

Connie B. Roth
Department of Physics, Emory University, Atlanta, GA, USA , e-mail: cbroth@emory.edu

Abstract:
Polymers exist in the glass state for a wide range of applications. The slow and limited crystallizability of polymers means that solid polymer materials are either wholly or in part glassy giving them great importance. The glass is a nonequilibrium amorphous state that occurs because the cooperative molecular dynamics become kinetically trapped on cooling as the available thermal energy for molecular motion decreases. This chapter aims to provide the reader with a molecular picture of what this packing frustration that causes glass formation means for polymers. Experimental considerations for accurately measuring the glass transition temperature T_g given this nonequilibrium nature will be discussed. Basic concepts underpinning theoretical efforts to model the glass transition will be summarized to provide the reader with a lexicon and paradigm for understanding different approaches used in the field to capture the main characteristics of glasses. Current research areas of interest in polymer glasses will be briefly outlined. Hopefully this chapter will provide the beginning investigator a starting point for their own studies.

Keywords: glasses, nonequilibrium dynamics, thermodynamics, kinetics, measurement

1. Glass Transition by Kinetic Arrest

Let us start by considering the dynamics polymers have in their equilibrium liquid state above the glass transition temperature T_g. In the melt, polymers have a broad range of relaxation times, moving primarily by bead-spring Rouse dynamics, as well as reptation in entangled systems. Many smaller scale vibrational and rotational motions are active as well. For small

molecules or short unentangled polymer chains, the glass transition represents the dynamical arrest of viscous flow. However, for polymers with high enough molecular weights that cause entanglements, viscous flow only really occurs at long times at temperatures sufficiently far above the glass transition, i.e., for times greater than the reptation time. For these high molecular weight systems, as the glass transition temperature is approached on cooling the polymer material will behave as a rubbery viscoelastic melt with local bead-spring Rouse modes between entanglement points and other more local segmental relaxations keeping molecular configurations in equilibrium. Outside of strong chain distortions that would relax quickly by chain retraction, the overall global conformation of the chain does not particularly impact the glass transition. Thus, for high molecular weight polymers, the glass transition does not represent the arrest of viscous flow of the entire chain, which has already effectively stopped, but the dynamic arrest of more local cooperative segmental motions. The length scale of these cooperative segmental dynamics are comparable to those of small molecules such that the polymer glass transition exhibits many of the same characteristics of other glass formers. Figure 1 graphs a representative plot of the modulus on a logarithmic scale as a function of temperature showing how the rubbery entanglement plateau effectively separates

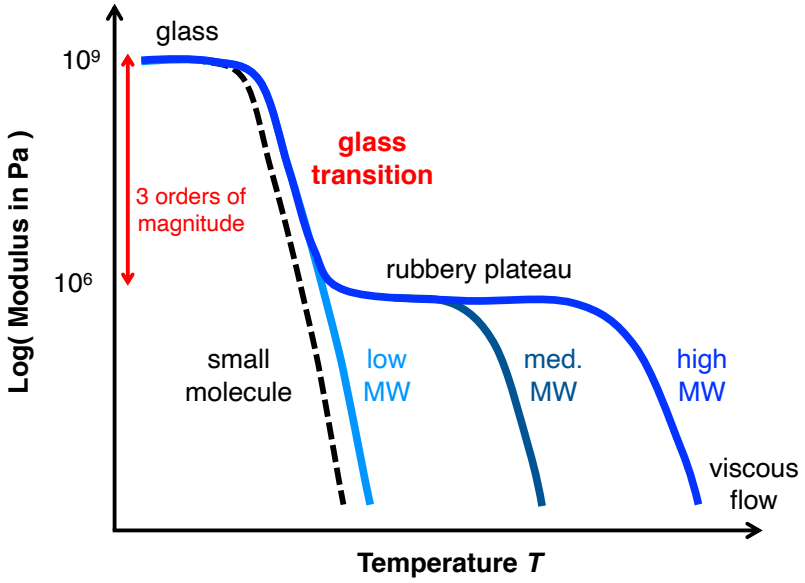

Figure 1 Representative plot of the logarithm of modulus as a function of temperature T comparing high, medium, and low molecular weight polymers with small molecules. For entangled polymers, the rubbery plateau effectively separates viscous flow from the glass transition. The modulus increases by approximately three orders of magnitude on cooling through the glass transition from the rubbery plateau to the glass state.

viscous flow from the glass transition in high molecular weight polymers. The principles of time-temperature superposition would shift the scale of the horizontal axis, but the relative difference between flow and T_g would remain. Below T_g only small scale vibrational and rotational motions remain active; the molecules are effectively locked into place resulting in a high gigapascal modulus.

Crystallization in polymers is relatively easy to avoid. The comparatively slow dynamics of polymers makes it easy to bypass crystallization as only modest cooling rates are needed to prevent polymer molecules from having sufficient time to order into a crystalline state. In contrast, higher cooling rates are usually needed to avoid crystallization of small molecules, and extreme cooling rates are required to glassify metals or water. Even if crystallization does occur in polymers, the material is typically only semi-crystalline with somewhere between 10–80 % crystalline content interconnected by amorphous domains. There are also many polymers for which stereo-irregularities in their chemical composition prevent molecular packing into an ordered crystal state. For the purposes of this chapter, we will focus solely on the glass state assuming crystallization has been avoided either by cooling fast enough to not give it enough time to occur, or the irregular (atactic) molecular structure of the polymer prevents it from ever occurring.

Figure 2 depicts a schematic plot of volume V as a function of temperature T that allows us to define several characteristics of glass formation. Above the glass transition in the liquid state, the volume-temperature curve is linear with a slope reflecting the thermal expansion of the material, $\alpha_V(T) = \frac{1}{V}\left(\frac{\partial V}{\partial T}\right)\Big|_P$, at constant pressure P. At high temperature, lots of extra "free" volume is available for the molecules to easily move around and slide past each other. On cooling, this extra space decreases and molecular mobility becomes more hindered. Below the crystallization temperature T_m, assuming the system has not crystallized, we refer to the system as being in a supercooled state.

In this supercooled state, the system is still in equilibrium, but the molecular dynamics begin slowing quite drastically. For polymers, the temperature dependence of the viscosity $\eta(T)$ in this regime is often characterized by the Williams, Landel, and Ferry (WLF) equation:

$$\log\left[\frac{\eta(T)}{\eta(T_{\text{ref}})}\right] = -\frac{C_1(T - T_{\text{ref}})}{C_2 + (T - T_{\text{ref}})}, \tag{1}$$

where T_{ref} is a reference temperature, and C_1 and C_2 are tabulated polymer dependent parameters. In the glass literature, the temperature dependence is typically characterized using the mathematically equivalent Vogel, Fulcher, Tammann (VFT) equation:

$$\eta(T) = \eta_0 \ \exp\left(\frac{B}{T - T_0}\right), \tag{2}$$

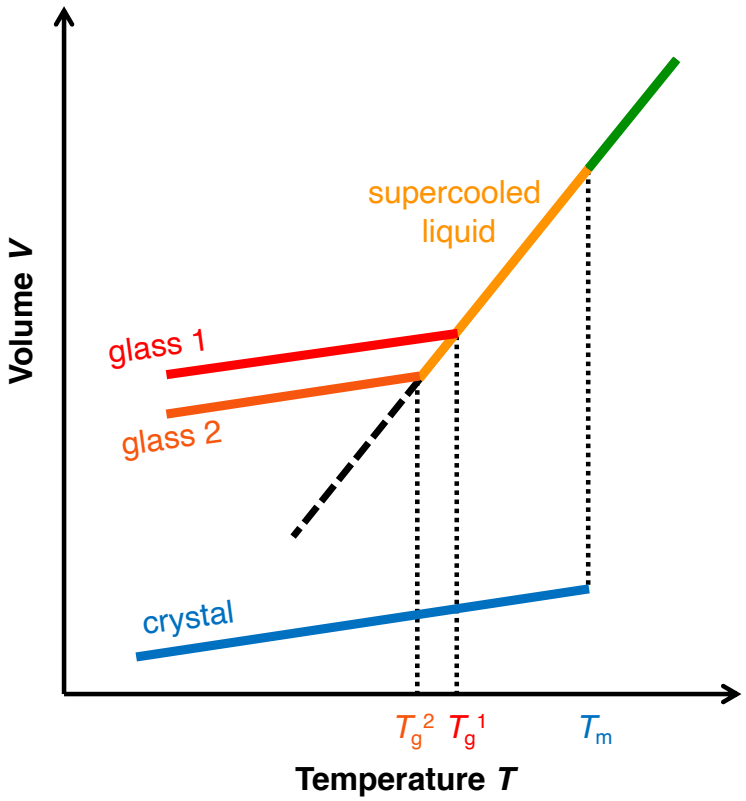

Figure 2 Volume V as a function of temperature T showing a polymer forming a glass on cooling at the glass transition temperature T_g^1, or T_g^2 on cooling at a slower rate, assuming crystallization at T_m does not occur. The thermal expansion (proportional to slope) of the glass state is typically the same as that of the crystalline state.

where the Vogel temperature $T_0 \simeq T_g - 50$ K, and B and η_0 are again material dependent parameters. This super-Arrhenius slowing in molecular dynamics on cooling continues for ≈50–100 K, over which the dynamics slow by ≈10–14 orders of magnitude, until which point the system just freezes into place at the glass transition temperature T_g. At a given cooling rate, the system was unable to molecularly rearrange into an equilibrium conformation at this new temperature before being cooled further.

The thermal expansion in the glass state is approximately the same as that in the crystalline state because the same localized segmental vibrations are still occurring. However, instead of the molecules being locked into an ordered equilibrium crystalline state, they are locked into a random, amorphous nonequilibrium state. Obviously because of this random packing, the volume of the glass state is higher than that in the ordered crystalline state. At a microscopic level, the molecules in the glass state are effectively frozen into place in essentially the same random configuration they had in the liquid state, except their density is slightly higher because there is no longer enough extra free space for the molecular units to move around in any meaningful way. In fact, one of the great mysteries of the glass transition is that if one could look at a picture at the molecular level of that for a glass and for a liquid,

we do not yet have the ability to discern simply from this static arrangement of molecules which one is able to move (i.e., in its liquid state) and which is frozen in place (i.e., in its glass state). This search for a link between the structure of a glass and its dynamics is one of active research (1).

The glass transition is often referred to as a kinetic transition because if one cools faster, the system will fall out of equilibrium sooner at a temperature T_g^1, forming a glass with a higher volume. If the system is cooled more slowly, the molecular configurations can continue to equilibrate for longer on cooling, falling out of equilibrium and forming a glass at a lower temperature T_g^2, with a corresponding lower volume. This difference in T_g with cooling rate is actually not particularly large with an order of magnitude increase in cooling rate usually only shifting T_g by 3–5 K at most (2). However, for all practical purposes, the glass transition occurs because of the kinetic arrest of molecular motion on cooling causing the material to fall out of equilibrium at some temperature T_g, effectively freezing into place. Theoretically, one wonders if we could hypothetically cool infinitely slowly, not allowing the system to fall out of equilibrium, would a true thermodynamic glass transition occur at some finite temperature? If so, would this correspond to some "ideal glass" state that exists at a very low temperature? We will return to such considerations when we discuss theoretical aspects as these fundamental questions underpin how the glass transition is modeled.

The nonequilibrium nature of the glass state achieved through a kinetic transition is not stable, especially when formed by cooling quickly. Because the nonequilibrium glass state has a higher volume than the equilibrium state, the system strives to densify. The limited mobility of the essentially frozen molecules in their glass state means this densification occurs very slowly, on a logarithmic time scale. Over time this structural relaxation changes the glass state such that it will become slightly denser. However, what is more significant is the host of other property changes that occurs during this physical aging such as an increase in modulus, an increase in brittleness, and a decrease in permeability. It is often one of these other property changes during physical aging that ultimately leads to failure of the material.

The amorphous molecular structure of the glass state gives glasses many of their distinctive properties. The lack of crystalline ordering means light is not scattered by an ordered molecular structure leaving glasses transparent. In addition, without molecular ordering there can be no crystalline defects that are usually weak points in the structure. Polymer glasses are typically known for being strong and tough materials, and in many cases exhibit considerable ductility. Thus, their applications as strong, transparent materials abound.

2. Microscopic Molecular Picture of the Glass Transition

The challenge with understanding glass behavior is the immense slowing down of dynamics that occurs in the supercooled regime while the system is still in equilibrium. Over a temperature range of 50–100 K as the glass transition is approached from above, the dynamics slow by 10–14 orders of magnitude. The kinetic arrest that then occurs at T_g leading to a nonequilibrium glass is simply the inevitable consequence of the dynamics becoming too slow to equilibrate on any reasonable timescale. At its most fundamental, we believe this dynamical slowing down results from the onset and growth of cooperative motion of molecular units on cooling.

At high temperature, molecular units are free to slide past each other with ease. Relaxation times in this regime are typically characterized by a simple Arrhenius temperature dependence

$$\tau \propto \exp\left(\frac{E_a}{k_B T}\right), \tag{3}$$

with a temperature independent activation energy E_a characterizing the viscous frictional forces (k_B is Boltzmann's constant). As less and less thermal energy is available for molecular activation on cooling, the relaxation times slow. In analogy with Equation 3, the relaxation time τ_α of these cooperative motions are often written as:

$$\tau_\alpha \propto \exp\left[\frac{E_a(T)}{k_B T}\right], \tag{4}$$

where the effective activation energy $E_a(T)$ of the system now increases with decreasing temperature. Several successful theories have been designed around treating $E_a(T) \propto zE_a^*$ with z corresponding to the growing number of units undergoing collective motion on cooling and E_a^* as a temperature-independent activation energy scale (3–5).

The designation of τ_α to refer to the cooperative motion associated with the glass transition is simply because it is the first relaxation time to freeze out on cooling, while more local processes that continue to lower temperatures are designated τ_β, τ_γ, etc (2). For polymers, τ_β would typically refer to a local segmental relaxation of order a couple of monomers, while τ_γ might represent some side group rotation (6).

Cooperative motion refers to molecular units needing to move collectively together for motion to occur. It is typically associated with some packing frustration preventing individual units from sliding past each other as the system densifies on cooling. For polymers, this packing frustration occurs at the cooperative segmental level encompassing several to many monomers. Principally, this packing frustration in polymers limiting mobility is not caused by

chain connectivity. The cooperative motion associated with the glass transition in polymers involves monomers from multiple different chains. A simple analogy can be made to a mosh pit where a crowd of dancers is so tightly packed that independent motion becomes extremely limited. In such a scenario, it matters little if these dancers were to hold hands forming long chains, motion would still be primarily limited by your immediate neighbors regardless of whether they were connected to your chain or not. It is for this reason that polymers exhibit many of the same characteristics as other glass formers like small molecules. The cooperative motion limiting mobility at the glass transition in polymers involves segmental units, which have roughly the same size scale as small molecules.

There are still open questions about the precise mapping of individual monomers for a given polymer chemical structure to the specific segmental units that determine this collective motion, as well as how chain ends may alter this. One recent successful attempt has used the Kuhn length, which characterizes the local flexibility of the chain, to map several different polymer chemical structures to effective molecular units that then undergo cooperative motion together on cooling (7).

The field of glasses refers to cooperatively rearranging regions (CRRs) whose size $\xi_{\mathrm{CRR}}(T)$ reflects the region of the system undergoing collective motion together. The term dates back to the 1965 theory of Adam and Gibbs that introduced the idea of CRRs in reference to the size of a cooperative region of particles whose transition probability for activated motion followed a form similar to Equation 4, rationalized by the decrease in available configuration entropy on cooling (3). Figure 3 tries to illustrate this concept of a growing CRR length scale $\xi_{\mathrm{CRR}}(T)$, emphasizing that a given CRR region includes molecular units from multiple polymer chains. A CRR has historically been conceptualized as spherical, thus for simplicity, this cartoon draws circles to indicate the CRR region. However, more recent efforts to visualize cooperative motion within computer simulations and colloidal glasses have instead observed more string-like shapes for CRRs (5, 8). By necessity these experiments and computer simulations observing string-like collective motion are effectively at a high temperature well above T_{g}. Theoretical efforts suggest that the shape of the CRRs likely vary with temperature, being more fractal or string-like at high temperatures and then becoming more compact and spherical at lower temperatures (9, 10). Note that when this string-like collective motion is observed in bead-spring simulations of polymers, the string-like motion of beads does not follow the connectivity of the chain (springs), but are similar to motions observed in simulations of unconnected Lennard-Jones spheres.

When trying to determine a size scale for the CRR, $\xi_{\mathrm{CRR}}(T)$, this is typically done assuming a spherical shape for the CRR where the CRR volume $V_{\mathrm{CRR}} = \xi^3_{\mathrm{CRR}}$. Experimentally

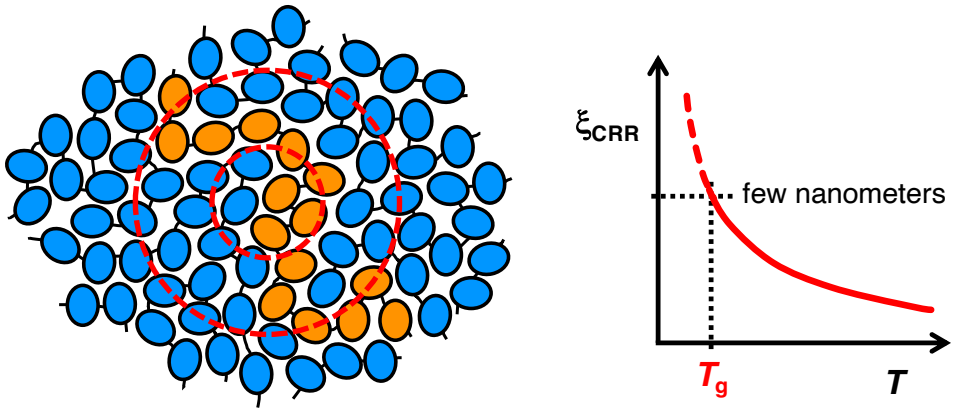

Figure 3 Illustration of the concept of a cooperatively rearranging region (CRR) whose size $\xi_{\mathrm{CRR}}(T)$ is believed to grow with decreasing temperature. The segmental units undergoing collective motion together because of packing frustrations do not necessarily correspond to the same molecular chain.

there have been several attempts to measure such an effective CRR size, where results typically give a size of around a few nanometers for $\xi_{\mathrm{CRR}}(T_{\mathrm{g}})$ at the glass transition. There has even been some indication of $\xi_{\mathrm{CRR}}(T)$ growing with decreasing temperature as T_{g} is approached from above (11–13). One approach for estimating a CRR size that has been used frequently for polymers is the Donth method where a CRR volume size is obtained from the step-change in heat capacity at T_{g}:

$$V_{\mathrm{CRR}} = \xi_{\mathrm{CRR}}^3 = k_B T_{\mathrm{g}}^2 \frac{\Delta(1/C_V)}{\rho(\delta T)^2}, \tag{5}$$

where $\Delta(1/C_V)$ is the reciprocal of the heat capacity step change at T_{g} at constant volume, ρ is the mass density, and $(\delta T)^2$ is the mean-square temperature fluctuation of an average CRR volume, a measure of the rate dependence of the transition, evaluated at T_{g} (14, 15).

This idea of some growing length scale of activated dynamics along the lines of Equation 4 is central to how we understand the strong slowing in dynamics that leads to the glass transition. Equation 4 is mathematically equivalent to the VFT equation (Equation 2 as $\tau_\alpha(T) \propto \frac{\eta(T)}{G_\infty}$), an empirical equation dating back to the 1920s, historically used to fit experimental data describing the temperature-dependent relaxation time of glasses. To highlight the non-Arrhenius character, such $\tau_\alpha(T)$ data are typically plotted on so-called Arrhenius plots of $\log(\tau_\alpha)$ versus $1/T$, where a simple Arrhenius process following Equation 3 would show as a straight line, while data following Equations 2 or 4 would be a curve whose tangent reflected the changing (temperature-dependent) effective activation energy. Figure 4

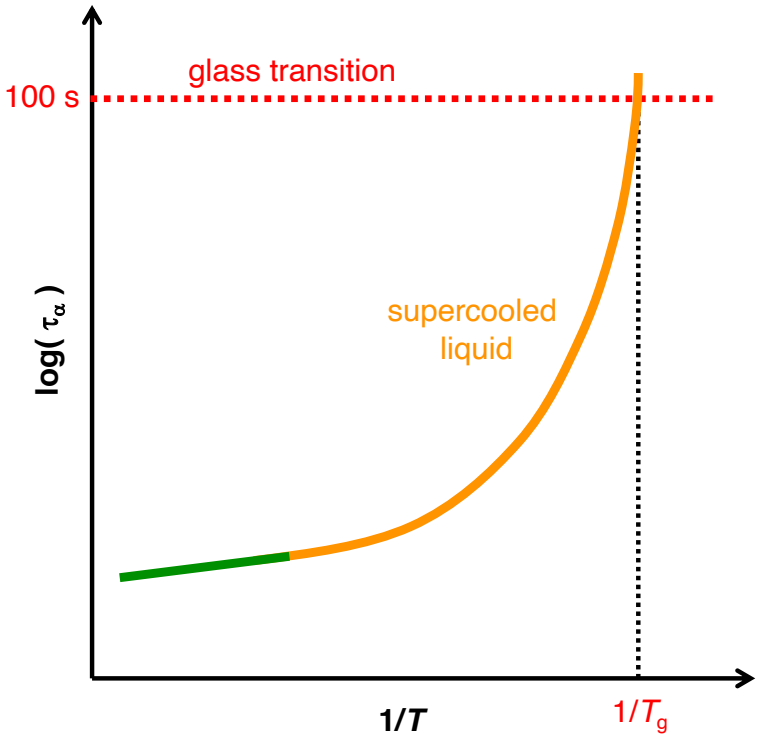

Figure 4 Schematic of an Arrhenius plot frequently used to graph the relaxation time for cooperative motion of glasses $\tau_\alpha(T)$ the curvature highlights its non-Arrhenius character following either Equation 2 or 4. A common definition for T_g is when the relaxation $\tau_\alpha(T_g) = 100$ s.

illustrates the basic features of such an Arrhenius plot, where a commonly used definition for T_g is when the relaxation time $\tau_\alpha(T)$ has grown to 100 s.

The rate at which the $\log(\tau_\alpha)$ curve passes through the glass transition at T_g was quantified by Angell as the concept of fragility m of a glass,

$$m = \left. \frac{d \log \tau_\alpha}{d(T_g/T)} \right|_{T=T_g}, \tag{6}$$

defined as the slope of the $\log(\tau_\alpha)$ versus $1/T$ plot at T_g (16). Most polymers are considered fragile (17, 18), showing a more non-Arrhenius-like behavior, whereas strong glass formers show a more Arrhenius-like behavior. (Note that these terms fragile and strong do not have any bearing to the material's modulus or strength.)

Beyond cooperative motion, another key characteristic of the molecular dynamics in the supercooled regime leading to the glass transition is dynamic heterogeneity. Local packing frustrations result in local regions of the material ξ_i with vastly different relaxation times τ_i such that the global average relaxation time of the material represents a sum of these many different local relaxations (19)

$$\langle \tau \rangle = \sum_i \xi_i \exp\left(-\frac{t}{\tau_i}\right). \tag{7}$$

This sum of many regions with different single exponential decays in relaxation time shows up experimentally as a stretched exponential with exponent β_{KWW} between 0 and 1, called the Kohlrausch–Williams–Watts (KWW) function,

$$\langle \tau \rangle = \xi_{\text{av}} \exp \left[- \left(\frac{t}{\tau_{\text{av}}} \right)^{\beta_{\text{KWW}}} \right]. \tag{8}$$

In addition, not only is the material spatially heterogeneous with this broad distribution in relaxation times, but also temporally heterogeneous, meaning over time locally fast regions will become slow and locally slow regions will become fast, as small shifts in the molecular units redistribute packing frustrations (19). Figure 5 schematically illustrates this spatial and temporal heterogeneity where a collection of local regions with a given set of relaxation times $\tau_1 < \tau_2 < \ldots < \tau_6$ at one time, exhibits a different set of relaxation times at a later time.

It is this non-homogeneousness within the material that leads to the breakdown of other relations that are common to homogeneous liquids (20). For example, decoupling of translational and rotational motions within supercooled liquids occurs as a consequence of how these different dynamics sample the broad distribution of relaxation times in dynamically heterogeneous materials. Microscopically, the mean-squared linear displacement

$$\lim_{\Delta t \to \infty} \left\langle \Delta \vec{r}^2(\Delta t) \right\rangle = 6 D_{\text{T}} \Delta t \tag{9}$$

characterizes the translational diffusion coefficient D_{T}, while the mean-squared angular dis-

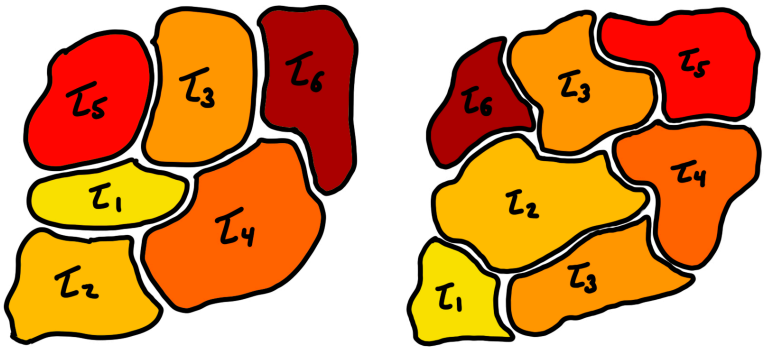

Figure 5 Illustration of dynamic heterogeneity within supercooled liquids showing both spatial heterogeneity with local regions exhibiting a range of different relaxation times $\tau_1 < \tau_2 < \ldots < \tau_6$ at one given time (left), as well as temporal heterogeneity, where at some time later after microscopic rearrangements have locally changed packing frustrations, a shifted set of local regions exhibit a different set of relaxation times (right).

placement

$$\lim_{\Delta t \to \infty} \left\langle \Delta \vec{\phi}^2(\Delta t) \right\rangle = 6 D_{\mathrm{R}} \Delta t \tag{10}$$

characterizes the rotational diffusion coefficient D_{R} (21). In supercooled liquids, it is the rotational diffusion coefficient $D_{\mathrm{R}}(T)$ that continues to scale with the viscosity $\eta(T)$, while the translational diffusion coefficient $D_{\mathrm{T}}(T)$ shows a weaker temperature dependence (20, 21). Thus, many of the relations one takes for granted for simple liquids may no longer apply to the supercooled liquid regime because of dynamic heterogeneity.

3. Measurement Implications of Glasses Being a Nonequilibrium State

Now that we have a good understanding of what occurs at the molecular level to cause the glass transition, let us consider the implications of this kinetic transition from a measurement perspective. The glass state formed on cooling depends on the rate at which the material is cooled because the ability of the molecular relaxations to maintain an equilibrium configuration depends on its ability to sample all possible configurations (ergodicity) prior to being cooled further. Cooling the material more rapidly will cause the molecular structure to lose this ability to maintain ergodicity at a higher temperature, falling out of equilibrium and arresting into a molecular structure with a higher volume (as was shown in Figure 1). This glass structure with poor packing will persist to lower temperature, unable to fully relax its frozen structure. Thus, the properties of the glass state formed are intimately connected to how the glass was cooled, i.e., how the glass was vitrified. A measurement of the glass transition done on heating will sample the state of this frozen glass structure that was formed and any evolution it has undergone in the glass state since vitrification.

The frozen-in nonequilibrium glass state that was formed does continue to have a thermodynamic driving force towards equilibrium. However, the limited thermal energy available in the glass state is insufficient to overcome the energy barriers required to cause cooperative relaxations such that molecular motions are limited to smaller scale rearrangements. Over a long time such smaller scale rearrangements do lead to slow densification of the material on a logarithmic timescale. This kinetic evolution of thermodynamic state variables such as volume and enthalpy of the nonequilibrium glass is referred to as structural recovery. Physical aging refers to the broader range of material property changes that accompany this process. Significant increases in modulus, brittleness, and loss of permeability can occur from physical aging, and are often responsible for the ultimate failure of the material. This slow evolution of the glass structure over time also implies that on reheating the glass state sampled can be different than what was originally formed on vitrification depending on how

long the glass has been held below its glass transition temperature. This thermal history of the material, since it was last in equilibrium above T_g, is an important factor to keep track of when making measurements of glasses.

3.1. Considerations When Measuring the Glass Transition

As the glass transition is by definition the falling out of equilibrium of the material on cooling, then a measurement of the glass transition temperature T_g is only formally defined on cooling. However, many measurement methods necessitate or routinely measure the glass transition on heating. Under these circumstances it is important to carefully control the thermal history of the sample.

Technically a measurement of the glass transition temperature on heating is a measure of the fictive temperature T_f of the glass. The fictive temperature T_f is defined as the temperature where an extrapolation along the glass line intersects with the equilibrium liquid line, and as such T_f is considered a measure of the frozen structure of the glass state. The measure of fictive temperature T_f on heating approximates the glass transition temperature T_g that would be measured on cooling when the heating rate matches the cooling rate that the glass was formed at, and provided that minimal time was spent in the glass state to avoid physical aging of the material (22–24). Under these measurement protocols, the glass line traced on heating will follow the glass line formed on cooling, giving a good measure of the glass transition temperature T_g usually within 1 K.

Figure 6 illustrates the difference that can arise between T_g measured on cooling and T_f measured on heating for a glass that has undergone physical aging. Enthalpy is lost over time as physical aging progresses resulting in a lower enthalpy glass line that is followed on heating, compared with the glass line that was traced out on cooling. This lower (aged) glass line intersects the equilibrium liquid line at a lower temperature resulting in a T_f that is less than T_g. There is also an extension of this lower glass enthalpy curve on heating that persists above T_g until the sample is fully able to regain equilibrium. This leads to what is commonly referred to as an enthalpy overshoot in a differential scanning calorimetry (DSC) heat-flow curve, where the size of the overshoot peak increases with increasing physical aging. Enthalpy overshoots can also result from differences in cooling and heating rates in DSC measurements (22). For example, when the sample's cooling rate is much slower than its subsequent heating rate, the glass will effectively age during the cooling process resulting in an overshoot on heating. Volumetric measurements such as ellipsometry can also show similar overshoots from physical aging, in this case in the thermal expansivity (25).

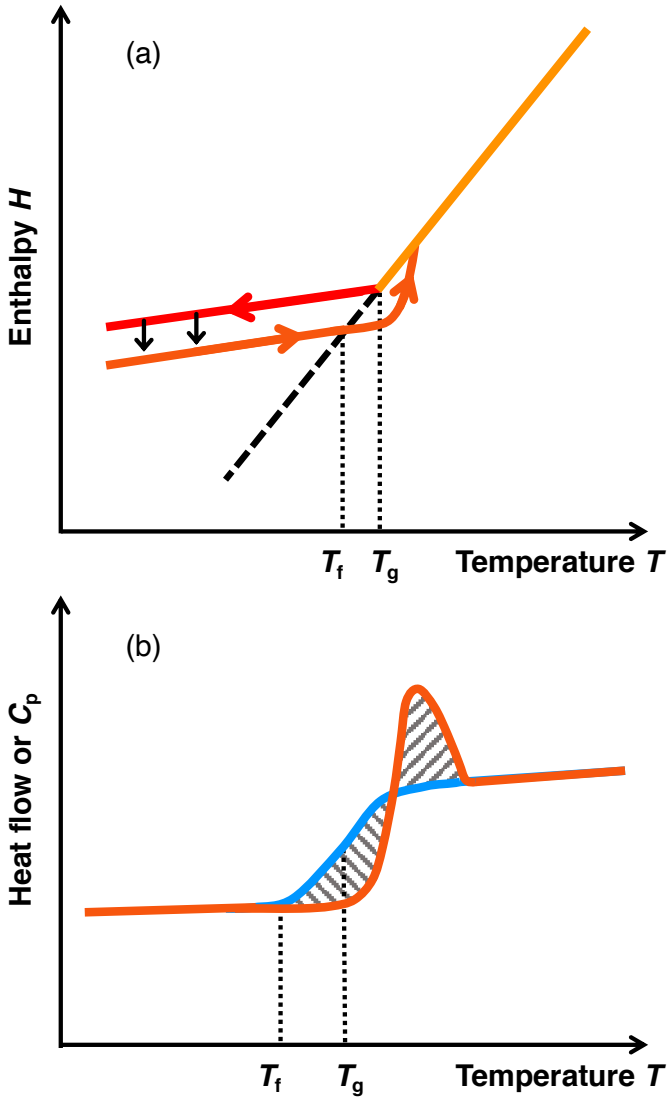

Figure 6 (a) Comparison of the enthalpy curves traced on cooling and subsequent heating after physical aging has occurred. The fictive temperature T_f measured on heating is defined as the temperature at which the glass line on heating intersects with the equilibrium liquid line. (b) Corresponding heat capacity curve obtained from the temperature derivative of the enthalpy, where the equal area construction between the aged $C_p^{\text{aged}}(T)$ (orange) and unaged $C_p^{\text{unaged}}(T)$ (blue) curves used to identify T_f based on Equation 11 is illustrated.

For differential scanning calorimetry, the measured heat flow curve corresponds to the heat capacity, which at constant pressure is the temperature derivative of the enthalpy, $C_p(T) = \left(\frac{\partial H}{\partial T}\right)\Big|_P$. Determination of the fictive temperature T_f from DSC heat-flow curves are best done with an equal area construction (26). Perhaps the most straightforward definition conceptually is the Richardson method (27) that defines the fictive temperature T_f based on the temperature at which the net difference in heat capacity between the aged and unaged $C_p(T)$ curves integrates to zero:

$$\int_{T_f}^{T \gg T_g} \left[C_p^{\text{aged}}(T) - C_p^{\text{unaged}}(T) \right] dT = 0. \tag{11}$$

This equates the enthalpy difference $\Delta H = \int \Delta C_p(T) dT$ between the aged heat capacity

curve $C_p^{\text{aged}}(T)$ above and below the unaged curve $C_p^{\text{unaged}}(T)$. The areas corresponding to this equal area construction are schematically illustrated in Figure 6b. Alternatively, the Moynihan method (23, 24, 28) does not require the separate measurement of the unaged heat capacity curve. This equal area construction utilizes the extrapolated liquid and glass lines as the baseline reference:

$$\int_{T_f}^{T \gg T_g} \left[C_p^{\text{liquid}}(T) - C_p^{\text{glass}}(T) \right] dT = \int_{T \ll T_g}^{T \gg T_g} \left[C_p^{\text{aged}}(T) - C_p^{\text{glass}}(T) \right] dT \qquad (12)$$

where the limits indicate that the liquid and glass lines need to be measured far enough away from the transition to be well defined.

The glass transition corresponds to the dynamic arrest of a distribution of time scales. As such, the breadth of the transition can easily span 10–20 K. Different experimental techniques will then naturally identify different parts of this broad transition as the specific glass transition temperature T_g reported. This will depend on the conventions of which part of the transition is taken as the T_g value, for example the peak in the loss modulus $G''(T)$ measured at a given frequency and cooling rate. Thus, it is not unusual for the reported T_g of a given polymer to differ by several degrees across measurements by different experimental techniques.

3.2. Physical Aging: Stability of the Glassy State

The slow evolution of the nonequilibrium glass state is characterized by several markers of physical aging. Thermodynamically this structural recovery manifests as a decrease in enthalpy as shown in Figure 6, as well as volume. In Figure 2, both glass 1 and glass 2 will slowly evolve, decreasing in volume towards the extrapolation of the equilibrium liquid line (black dashed line). Because glass 1 was cooled faster, falling out of equilibrium at a higher volume, its rate of volume decrease will be faster than that of glass 2 that is closer to the equilibrium state. Glass 1 is less stable than glass 2.

This stability of the glassy state is most straightforwardly characterized by the evolution of intrinsic isotherms with time measured after a temperature quench from the equilibrium liquid state to some temperature in the glass state. The departure from equilibrium δ of the current state of the glass at a given time t relative to when the equilibrium liquid line is reached at $t \to \infty$ is defined (29) from either the volume as

$$\delta_V(t) = \frac{V(t) - V_\infty}{V_\infty} \qquad (13)$$

or enthalpy as

$$\delta_H(t) = H(t) - H_\infty \qquad (14)$$

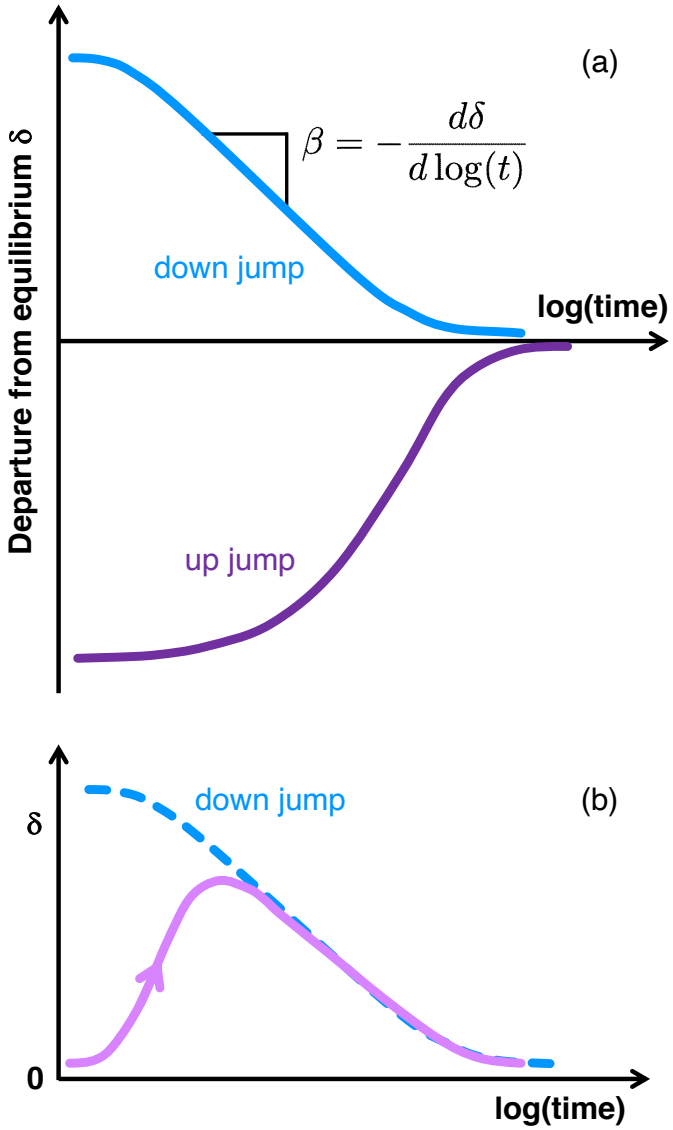

Figure 7 (a) Physical aging isotherms depicting the asymmetry of approach in the departure from equilibrium δ after a down or up jump of ΔT to the same aging temperature T_{age}. (b) Memory response in the departure from equilibrium δ illustrated, see text for description of the thermal history.

obtained from the growth in area of the enthalpy overshoot peak measured in a DSC heat flow curve on heating (29, 30). Figure 7a illustrates the full progression of the departure from equilibrium δ as a function of $\log(t)$ for a glass from its initial temperature quench at $t = 0$ to when it finally reaches equilibrium in the limit of $t \to \infty$. In practice, equilibrium can only be reached on reasonable time scales for temperature quenches at most several degrees below T_g (29, 31). Heroic experiments conducted for over a year have observed equilibrium being reached at an aging temperature 10 K below T_g (30). Thus, typically only a subset of the full curve shown in Figure 7a is measured experimentally.

The stability of the glass state is often characterized by measuring the physical aging rate β, as originally defined by Struik (32), determined as the slope of the departure from

equilibrium δ as a function of $\log(t)$ in the region where this is linear:

$$\beta = -\frac{d\delta}{d\log(t)}. \tag{15}$$

Interestingly, the volume relaxation rate β_V and the enthalpy relaxation rate β_H determined from volumetric or enthalpic measurements respectively, are not equivalent for a given polymer or across different polymers. At the same temperature below T_g, a given polymer can exhibit a higher volume relaxation rate β_V than another polymer that exhibits a higher enthalpy relaxation rate β_H than it (29). In general, polymers reach enthalpic equilibrium sooner than volumetric equilibrium. Thus, even though these different factors are connected to the same evolution process, there is a need to characterize various properties of the glass state to obtain a full description. Similar definitions of a physical aging rate have been developed for a range of other measurable properties (29, 33, 34).

The characteristic logarithmic time dependence associated with physical aging across all glass formers is emblematic of local "rattling" motions leading to intermittent structural relaxations that become exponentially less likely to occur as time progresses (35, 36). There is an intricate, interdependent link between dynamics and structure in glasses. Struik originally described this connection in terms of free volume v_f. The available free space between the packing of molecular units allows for a certain degree of molecular mobility that leads to a decrease in the system's volume with time. This in turn reduces the available free space resulting in a reduction in the mobility and therefore a reduction in the speed at which the system's volume decreases, getting progressively slower as time proceeds (32):

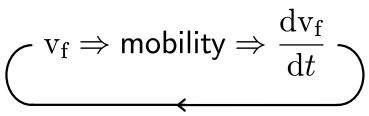

Such free volume ideas have been extensively used to describe physical aging in gas permeation studies (37, 38). In recent years, we are more likely to describe the physical aging process in terms of the evolution of the system down an energy landscape where the number of available configurations and corresponding mobility decreases as the system moves lower in the landscape (39–41). For aged systems, the fictive temperature T_f is used to describe the effective temperature of the glassy system, different from the actual thermodynamic temperature T, as the system's fictive temperature $T_f < T$ will include the reduced mobility associated from structural factors. As the molecular structure of the material becomes more ideally packed, there is less ability for the molecules to move around, locking in its structure and reducing the dynamics.

A classic set of experiments characterizing different aspects of the physical aging response were devised by Kovacs and have come to be known as the Kovacs signatures (42, 43). The first is the classic down jump intrinsic isotherm response after a temperature quench from the equilibrium liquid state to some aging temperature T_{age}. This is the one that was already discussed above in Figure 7a. The second is the isotherm response measured after an up jump to the aging temperature T_{age} starting from a system that was already relaxed to equilibrium at a temperature $T < T_{age}$. Obviously for practical reasons there is a limited temperature range just below T_g where this can feasibly be done. Figure 7a also includes the isotherm response from such an up jump to the same aging temperature T_{age} that the down jump intrinsic isotherm response is shown, with both the up and down jumps experiencing the same ΔT size of jump. Both curves show the departure from equilibrium $\delta \rightarrow 0$ as equilibrium at T_{age} is eventually reached. However, there is asymmetry to the approach as $\delta \rightarrow 0$ from an up jump compared with the down jump. The up jump response is characterized by an initial delay were the material must first slowly decompress and unlock its structure before its mobility can increase and evolve more quickly to the final equilibrium state $\delta = 0$. This is a classic signature demonstrating how the dynamics are impacted not only by the temperature, as both the down jump and up jump curves are at the same thermodynamic temperature T, but also by the current structure of the material that depends on its prior thermal history.

The third Kovacs aging signature is shown in Figure 7b. This experiment has a bit more complicated of a setup. We need to consider two aging temperatures T_{age1} and T_{age2} with $T_{age1} < T_{age2}$. The system is initially sent on a down jump aging to T_{age1}, but when the total volume or enthalpy line crosses the glass line at T_{age2}, the temperature is jumped immediately up to T_{age2}. The departure from equilibrium δ at this new aging temperature T_{age2} is zero, and in principle, one might think that δ will simply remain at zero as a function of time sitting now at T_{age2}. If the material had only a single relaxation time that is what would happen, but that is not what is observed. Instead a strong memory effect of the sample's thermal history is observed that provides a key signature demonstrating the material has a distribution of relaxation times. The classic response is shown in Figure 7b where first there is an increase in δ with time as the fast relaxations that had already aged below T_{age2} on their way to T_{age1} now uncompress. Eventually the curve joins that of the intrinsic isotherm response from a single down jump to T_{age2} as the slowest relaxations are finally now only making their way to equilibrium at T_{age2}. Similar Kovacs signatures have also been observed for concentration jumps using plasticizers (44).

4. Theoretical Concepts Used to Understand Glasses

Let us consider now some of the theoretical approaches used to model polymer glasses. Fundamentally the challenge with understanding glasses and the glass transition is that the phenomenon is based on collective, many body interactions that leads to a nonequilibrium state. Thus, our traditional statistical mechanics formulation that typically count pair-wise interactions to describe equilibrium systems is not up to this task. There are open questions in science currently in many areas related to many-body and nonequilibrium phenomena.

Many different theories have been proposed to explain the glass transition, too many to properly cover them all, even in a comprehensive review, and such an effort would quickly become outdated anyways. However, what is constructive to describe is broadly the various different theoretical approaches used to conceptualize and understand glasses. As a first categorization, there appears to be a separation of different approaches, as well as personal belief by theorists, about whether the glass transition is fundamentally rooted in an underlying thermodynamic transition or whether the phenomenon is purely kinetic (45, 46). This distinction may not seem so important to simple experimental measurements of T_g where the transition is experienced as a kinetic effect associated with the given cooling rate used. However, from a theoretical perspective, this distinction has important fundamental implications about the nature of entropy for a purely disordered system relative to that of an ordered crystal (47). This fundamental belief about the existence of an underlying thermodynamic transition influences the theoretical foundation by which the mathematical approach is formulated.

The main puzzle associated with the glass transition is the dramatic slowing down of dynamics by 10–14 orders of magnitude in timescales that occurs in the last 50–100 K on cooling before the system is finally unable to have enough molecular rearrangements to maintain equilibrium, ultimately forming a nonequilibrium glass at the glass transition temperature T_g (47). It is this dramatic slowing in dynamics, while the system is still in equilibrium, where most theoretical efforts are focused. As described above, the slowing down in this supercooled region is believed to arise from the onset of collective motion, which occurs at some upper temperature T_A, designated for the end of the Arrhenius temperature dependence. How one chooses to mathematically formulate these collective interactions varies considerably, with some approaches having a clear connection to the underlying molecular structure while others can be rather abstract.

An important concept used frequently to describe cooperative motion is the idea of caging and cage breaking. Let's consider the simple formulation of treating our material as a col-

lection of spheres. To start, we are not going to worry about connecting these spheres into chains to make polymers, which turns out not to be that important anyways. At high temperatures above T_A, these spherical particles can easily slide past each other behaving as a simple fluid. As we cool below T_A and cooperative motion sets in, the packing density of the spherical particles have increased such that if we focus on a single particle it appears caged by its neighbors on short time scales. Our particle must wait until its neighboring set of particles collectively shift enough to create a passage for our particle to escape this cage, ending up trapped in yet another temporary cage. Illustrated in Figure 8, this cage breaking event is considered to be an α-relaxation event occurring on average after a wait time τ_α, before which the particle is trapped rattling around within its cage. As the temperature decreases and the density of the system increases, the ability of the caging particles to shift enough to create such a passage for a cage breaking event to occur becomes less and less leading to a non-Arrhenius increase in the average waiting time $\tau_\alpha(T)$ between cage breaking events. Eventually, this $\tau_\alpha(T)$ timescale becomes so long that cage breaking events can no longer occur and the system is considered to be a glass.

Such a conceptual framework of cooperative motion into cage breaking events has been formulated many times into detailed theoretical models, and I am glossing over many details. Fundamentally, such a treatment is considered a mean-field treatment where the focus is usually on one particle of interest and the effect of all surrounding particles on that one particle is treated with some effective potential energy barrier that must be overcome for the

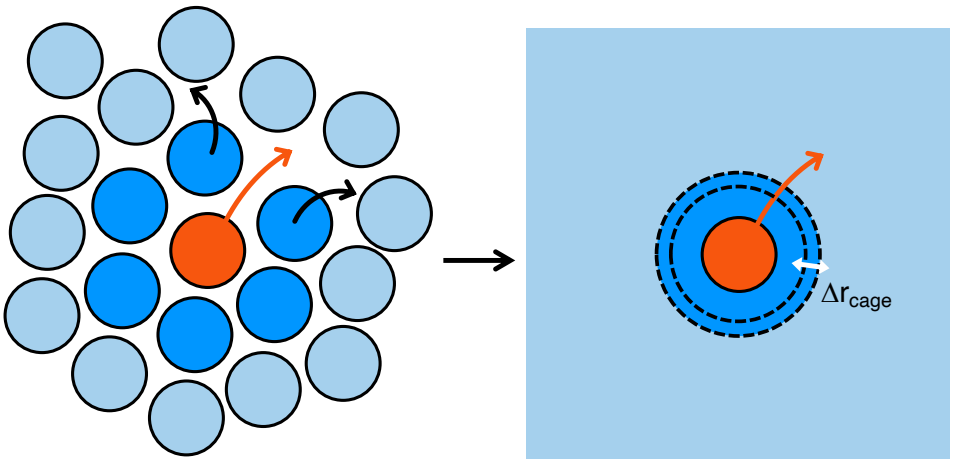

Figure 8 (left) Illustration of a cage breaking event triggered by the small shifting of neighboring spheres. (right) Mean-field representation where all the surrounding particles have been replaced with some effective potential defining the allowed fluctuation in cage size.

α-relaxation event to occur. Unsurprisingly, early models treating the system as simple hard spheres led to the glass transition occurring at too high a temperature (too low a density); soft particles have also been treated.

For the purposes of our discussion on polymers, an excellent formulation starting from this kind of conceptual framework has been developed by Schweizer and coworkers over several years. Recently, considerable advance has been made by including an additional energy barrier term for the cage breaking event that incorporates the local compressibility (elasticity) of the material surrounding the cage (48, 49). This Elastically Collective Nonlinear Langevin Equation (ECNLE) theory has been applied to several different polymers with surprising success, where the theory has been able to successfully predict the glass transition temperature T_{g}, the fragility m, and the average cooperative segmental relaxation time $\tau_\alpha(T)$ spanning approximately 10 orders of magnitude in timescale (7).

Remarkably, the ECNLE theory has no adjustable parameters, but instead uses a rather simple mapping to convert a polymer chain into a series of disconnected, noninterpenetrating spheres whose diameter is equal to the Kuhn length l_K of the polymer. Using this mapping, the chain length dependence of the glass transition temperature $T_{\mathrm{g}}(N)$ can be captured because the sphere size incorporates the chain length dependence of the polymer's flexibility through the characteristic ratio C_N as $l_K = C_N\, l_{bb}$, where l_{bb} is the average length of the backbone bond (7). The success of this theory treating polymers as comprised of a series of disconnected spheres reinforces the idea that the packing frustration causing the glass transition in polymers is not associated with chain connectivity, but instead the packing frustration is associated with the rigidity of local chain segments.

Other thermodynamic models have been proposed that also treat polymers as disconnected van der Waals spheres. Long and coworkers have explicitly treated the heterogeneity in glasses arising from density fluctuations as small domains with varying relaxation times, where the glass transition then arises from a percolation of slow domains across the material (50–52).

Another important theoretical concept that has seen considerable advances in recent years in the concept of free volume. The original formulation by Doolittle, which has long been contradicted by pressure dependent experiments, tried to explain the entire non-Arrhenius temperature dependence of the viscosity based solely on a free volume term. Instead, recent work by White and Lipson has completely revamped the formulation of free volume, demonstrating that volume and temperature act as two independent parameters controlling the cooperative segmental dynamics (53, 54). For example, data for numerous polymers

can be collapsed into a function of the form

$$\ln\left(\frac{\tau_\alpha}{\tau_{\text{ref}}}\right) = g(V) \times f(T), \tag{16}$$

where $g(V)$ and $f(T)$ represent independent functions in volume and temperature. Further, by modeling PVT data for different polymers, they are able to rigorously define the hard core volume V_{hc} representing the minimal closed-packed state of molecular packing for a given polymer (53–55). This allows for a nonambiguous definition of free volume $V_{\text{free}} = V - V_{\text{hc}}$ providing a formulation for the dynamics as

$$\ln\left(\frac{\tau_\alpha}{\tau_{\text{ref}}}\right) = \left(\frac{V_{\text{hc}}}{V_{\text{free}}}\right)\left(\frac{T^*}{T}\right)^b, \tag{17}$$

where τ_{ref}, T^*, and b represent material specific parameters. Thus, one can view this as the activation energy $E_a(T)$ in Equation 4 being proportional to $E_a(T) \propto \frac{1}{V_{\text{free}}}$ (54, 55).

There also exist purely kinetic models that can often be quite abstract, but benefit from being mathematically and computationally easier to apply to complex systems. Fundamentally they also ask the important question of what minimal factors are needed to capture the essential features associated with the glass transition. If the main features of the glass transition can be captured in a model with no phase transition in the thermodynamic equilibrium sense, does that imply that the glass transition is not a true thermodynamic transition? One example of such a model is the two-spin facilitated kinetic Ising model by Fredrickson and Andersen (56, 57). With only nearest-neighbor dynamical interactions and no equilibrium phase transition or inherent static correlation length, it is able to capture a number of features associated with the glass transition such as the broad distribution of relaxation times and eventual dynamic arrest into a glass state as the temperature parameter is reduced. More sophisticated kinetic models have been developed that make the connection to the material's properties less abstract. For example, Lipson and Milner have constructed a limited mobility model where individual domains can have three different mobility states based on their local free volume content (58). With the model only allowing for exchange of free volume between neighboring sites, large scale heterogeneous domains of mobility are still observed.

Finally, an important conceptual framework for understanding many-body interactions is the potential energy landscape (PEL) (39, 47, 59), originally proposed by Goldstein (60). This landscape picture treats the system in phase space where each location represents one configurational state of the system making the vertical coordinate the total potential energy of the system in that state. The horizontal coordinate actually represents a multidimensional

space over all degrees of freedom in the system. Visualization for even the simplest system is not feasible, which is why the PEL is typically represented by a two-dimensional cartoon drawing illustrating the complicated ruggedness of the landscape. The number of states (energy minima) at any given energy level is determined by the density of states based on the configurational entropy. This PEL representation treats dynamics of the system as an activated energy hoping process from one local minima to the next, where such transitions represent real space rearrangements of some small number of particles locally. Most such transitions are reversible, where the system explores a collection of local minima over a large number of these reversible transitions within a given metabasin. The treatment of many-body interactions in this framework then becomes about determining how the system evolves in this phase space, where relaxation of the system results from irreversible energy transitions from one metabasin to the next. Given the typically complex structure of the landscape these irreversible metabasin transitions can become probabilistically unlikely making larger parts of the configurational landscape inaccessible, and hence trapping the system in various nonequilibrium configurations.

5. Current Areas of Research in Polymer Glasses

This chapter has tried to provide the reader with a conceptual framework about how to understand polymer glasses. This understanding about the fundamental nature of the glass transition will hopefully inform the researcher about how to approach their experimental design for measuring the glass transition temperature T_g reliably given the material's thermal history. By explaining the basic idea behind various frameworks used to described glasses, the reader should be able to more easily follow the sometimes complex treatments of these topics they encounter in the literature. As an ending point to this chapter and a starting point for future research, we end here with a short summary of the many topics in polymer glasses that are currently under investigation.

For bulk polymer glasses there is still interest in the long studied time, temperature, and deformation behavior of the glass state under different thermal histories (61). As there is not a comprehensive theoretical treatment, characterization and modeling of the polymer glass response resulting from various processing and thermal histories of interest are still necessary (62). This is especially true for new processing methods that occur in the solid glass state. A long standing question with limited investigation is how the glass state varies with solvent or plasticizer content (44, 63). To what extent does this separate control parameter for increasing molecular mobility act similar or different from increasing the temperature. Are

glass states formed from concentration jumps equivalent to states formed from temperature jumps.

Much materials design now makes use of interfacial interactions to tailor the properties of the polymer. Everything from polymer nanocomposites to rubber toughening using glassy-rubbery interfaces, to thin films and nanoconfined geometries; multicomponent nanostructured materials are on the rise. After a couple of decades of intense research in these areas considerable understanding has developed about the nature of the free surface (64) and property changes in polymer thin films (65–67) and nanocomposites (68–70), including theoretical treatments. By no means is everything understood, there are still numerous outstanding issues to address, but enough understanding has occurred to develop some level of predictability and design use. For example, glasses with exceptional stability can be formed by harnessing the accelerated dynamics at the free surface to improved molecular packing (71), including recently in polymers (72).

Acknowledgements The author gratefully acknowledges support from the National Science Foundation Polymers Program (DMR-1905782) and Emory University, as well as many excellent conversations with colleagues and students.

Further Reading

G. B. McKenna and S. L. Simon. 50th Anniversary Perspective: Challenges in the Dynamics and Kinetics of Glass-Forming Polymers, *Macromolecules*, **50** (17), 6333–6361 (2017). doi:10.1021/acs.macromol.7b01014

C. B. Roth (Ed.), *Polymer Glasses*, CRC Press, (2016).

W. W. Graessley, *Polymeric Liquids & Networks: Dynamics and Rheology*, Garland Science, (2008).

Cited References

1. V. Bapst, T. Keck, A. Grabska-Barwińska, C. Donner, E. D. Cubuk, S. S. Schoenholz, A. Obika, A. W. R. Nelson, T. Back, D. Hassabis, and P. Kohli, Nature Physics **16**, 448 (2020).

2. R. Greiner and F. R. Schwarzl, Rheologica Acta **23**, 378 (1984).

3. G. Adam and J. H. Gibbs, Journal of Chemical Physics **43**, 139 (1965).

4. F. W. Starr, J. F. Douglas, and S. Sastry, Journal of Chemical Physics **138**, 12A541 (2013).

5. B. A. P. Betancourt, J. F. Douglas, and F. W. Starr, Journal of Chemical Physics **140**, 204509 (2014).

6. N. G. McCrum, B. E. Read, and G. Williams, *Anelastic and Dielectric Effects in Polymeric Solids* (John Wiley & Sons, New York, 1967).

7. S. Mirigian and K. S. Schweizer, Macromolecules **48**, 1901 (2015).

8. S. C. Glotzer, Journal of Non-Crystalline Solids **274**, 342 (2000).

9. J. D. Stevenson, J. Schmalian, and P. G. Wolynes, Nature Physics **2**, 268 (2006).

10. K. H. Nagamanasa, S. Gokhale, A. K. Sood, and R. Ganapathy, Nature Physics **11**, 403 (2015).

11. B. M. Erwin and R. H. Colby, Journal of Non-Crystalline Solids **307**, 225 (2002).

12. U. Tracht, M. Wilhelm, A. Heuer, H. Feng, K. Schmidt-Rohr, and H. W. Spiess, Physical Review Letters **81**, 2727 (1998).

13. S. A. Reinsberg, X. H. Qiu, M. Wilhelm, H. W. Spiess, and M. D. Ediger, Journal of Chemical Physics **114**, 7299 (2001).

14. E. Hempel, G. Hempel, A. Hensel, C. Schick, and E. Donth, Journal of Physical Chemistry B **104**, 2460 (2000).

15. E. Donth, Journal of Polymer Science Part B: Polymer Physics **34**, 2881 (1996).

16. C. A. Angell, Science **267**, 1924 (1995).

17. A. P. Sokolov, V. N. Novikov, and Y. Ding, Journal of Physics: Condensed Matter **19**, 205116 (2007).

18. K. Kunal, C. G. Robertson, S. Pawlus, S. F. Hahn, and A. P. Sokolov, Macromolecules **41**, 7232 (2008).

19. R. Richert, in *Structural Glasses and Supercooled Liquids: Theory, Experiment, and Applications*, edited by P. G. Wolynes and V. Lubchenko (John Wiley & Sons, 2012) Chap. Supercooled Liquid Dynamics: Advances and Challenges, pp. 1 – 30.

20. M. D. Ediger, Annual Review of Physical Chemistry **51**, 99 (2000).

21. K. V. Edmond, M. T. Elsesser, G. L. Hunter, D. J. Pine, and E. R. Weeks, Proceedings of the National Academy of Sciences **109**, 17891 (2012).

22. P. Badrinarayanan, W. Zheng, Q. Li, and S. L. Simon, Journal of Non-Crystalline Solids **353**, 2603 (2007).

23. A. K. T. Arellano and G. B. McKenna, Journal of Polymer Science Part B: Polymer Physics **53**, 1261 (2015).

24. C. T. Moynihan, A. J. Easteal, J. Wilder, and J. Tucker, Journal of Physical Chemistry **78**, 2673 (1974).

25. S. Kawana and R. A. L. Jones, European Physical Journal E **10**, 223 (2003).

26. E. Lopez and S. L. Simon, Macromolecules **49**, 2365 (2016).

27. M. J. Richardson and N. G. Savill, Polymer **16**, 753 (1975).

28. C. T. Moynihan, in *Assignment of the Glass Transition*, edited by R. J. Seyler (ASTM International, West Conshohocken, PA, 1994) pp. 32–32–18.

29. J. M. Hutchinson, Progress in Polymer Science **20**, 703 (1995).

30. Y. P. Koh and S. L. Simon, Macromolecules **46**, 5815 (2013).

31. S. L. Simon, J. W. Sobieski, and D. J. Plazek, Polymer **42**, 2555 (2001).

32. L. C. E. Struik, *Physical Aging in Amorphous Polymers and Other Materials* (Elsevier Scientific Publishing Company, Amsterdam, 1978).

33. E. A. Baker, P. Rittigstein, J. M. Torkelson, and C. B. Roth, Journal of Polymer Science, Part B: Polymer Physics **47**, 2509 (2009).

34. A. Shavit and R. A. Riggleman, Journal of Physical Chemistry B **118**, 9096 (2014).

35. P. Sibani, S. Boettcher, and H. J. Jensen, European Physical Journal B **94**, 37 (2021).

36. S. Boettcher, D. M. Robe, and P. Sibani, Physical Review E **98**, 020602 (2018).

37. Y. Huang and D. Paul, Polymer **45**, 8377 (2004).

38. J. Park and D. Paul, Journal of Membrane Science **125**, 23 (1997).

39. M. D. Ediger and P. Harrowell, Journal of Chemical Physics **137**, 080901 (2012).

40. A. Heuer, Journal of Physics: Condensed Matter **20**, 373101 (2008).

41. C. Rehwald, N. Gnan, A. Heuer, T. Schrøder, J. C. Dyre, and G. Diezemann, Physical Review E **82**, 021503 (2010).

42. G. B. McKenna and S. L. Simon, Macromolecules **50**, 6333 (2017).

43. A. J. Kovacs, Fortschr Hochpolym Forsch **3**, 394 (1963).

44. G. B. McKenna, Journal of Non-Crystalline Solids **353**, 3820 (2007).

45. L. Berthier and G. Biroli, Reviews of Modern Physics **83**, 587 (2011).

46. G. Biroli and J. P. Garrahan, Journal of Chemical Physics **138**, 12A301 (2013).

47. A. Cavagna, Physics Reports **476**, 51 (2009).

48. S. Mirigian and K. S. Schweizer, Journal of Physical Chemistry Letters **4**, 3648 (2013).

49. S. Mirigian and K. S. Schweizer, Journal of Chemical Physics **140**, 194506 (2014).

50. D. Long and F. Lequeux, European Physical Journal E **4**, 371 (2001).

51. S. Merabia and D. Long, European Physical Journal E **9**, 195 (2002).

52. S. Merabia and D. Long, Journal of Chemical Physics **125**, 234901 (2006).

53. R. P. White and J. E. G. Lipson, Macromolecules **49**, 3987 (2016).

54. R. P. White and J. E. G. Lipson, Journal of Chemical Physics **147**, 184503 (2017).

55. R. P. White and J. E. G. Lipson, Journal of Physical Chemistry B **125**, 10.1021/acs.jpcb.1c01620 (2021).

56. G. H. Fredrickson and H. C. Andersen, Physical Review Letters **53**, 1244 (1984).

57. G. H. Fredrickson and H. C. Andersen, Journal of Chemical Physics **83**, 5822 (1985).

58. N. B. Tito, J. E. G. Lipson, and S. T. Milner, Soft Matter **9**, 3173 (2013).

59. D. Wales, *Energy Landscapes: Applications to Clusters, Biomolecules and Glasses* (Cambridge University Press, Cambridge, 2004).

60. M. Goldstein, Journal of Chemical Physics **51**, 3728 (1969).

61. S.-Q. Wang, S. Cheng, P. Lin, and X. Li, Journal of Chemical Physics **141**, 094905 (2014).

62. G. A. Medvedev and J. M. Caruthers, in *Polymer Glasses*, edited by C. B. Roth (CRC Press, 2016) pp. 453 – 538.

63. G. B. McKenna, Journal of Physics: Condensed Matter **15**, S737 (2003).

64. M. D. Ediger and J. A. Forrest, Macromolecules **47**, 471 (2014).

65. C. B. Roth, J. E. Pye, and R. R. Baglay, in *Polymer Glasses*, edited by C. B. Roth (CRC Press, 2016) pp. 181 – 204.

66. B. D. Vogt, Journal of Polymer Science, Part B: Polymer Physics **56**, 9 (2017).

67. K. S. Schweizer and D. S. Simmons, Journal of Chemical Physics **151**, 240901 (2019).

68. S. K. Kumar, V. Ganesan, and R. A. Riggleman, Journal of Chemical Physics **147**, 020901 (2017).

69. L. M. Hall, A. Jayaraman, and K. S. Schweizer, Current Opinion in Solid State and Materials Science **14**, 38 (2010).

70. V. Ganesan and A. Jayaraman, Soft Matter **10**, 13 (2013).

71. M. D. Ediger, Journal of Chemical Physics **147**, 210901 (2017).

72. A. N. Raegen, J. Yin, Q. Zhou, and J. A. Forrest, Nature Materials **19**, 1110 (2020).